Effect of SMA Welding Electrodes on Mechanical and Corrosion of Low-Carbon Steel Joint

I.M. Dagwa[1], O. E. Malomo[2], B. Salihu[2], A. Mohammed[2], O. Saint[2], U. J. Abubakar[2]
[1]Department of Mechanical Engineering, University of Abuja, Nigeria
[2]Department of Mechanical Engineering, Ahmadu Bello University, Zaria, Nigeria
E-mail: supomalomo@yahoo.com

ABSTRACT
In this work, the effect of Shielded Metal Arc (SMA) welding electrodes on mechanical and corrosion of low carbon steel joint was investigated. Commonly used electrodes types (Sample A: J-Wheel; B: Oerlikon and C: J-Danish) by local welders and fabricators were selected. Welded samples were prepared into standard test samples for hardness, impact and tensile tests. Subsequently, standard facilities were used to determine the mechanical properties. The welded low carbon steel joint of these samples were immersed in test media (2.81 % NaCl solution) for some exposure period of time (504 hours), and their weights were taken at intervals of 72 hours to evaluate their weight loss and corrosion rate. The outcomes of mechanical properties evaluated were in the order: (Control>B>C>A) in terms of ultimate tensile strength, percent elongation and the hardness at 24 hrs were in the order of (Control >A=B=C) and (C>B> Control>A) respectively. While and hardness at 504 hours was (C>B> Control >A). Hence, Sample B weldment showed superior mechanical properties and corrosion resistance than Samples A and C. Uniform corrosion was observed on the exposed test coupons as corrosion rates were highest during the initial stages but gradually reduced with increased exposure time. It was apparent that improper choice of electrode type could affect the mechanical properties and corrosion rate of low carbon steel joints.

Keywords: Hardness, Impact, Tensile, Weight loss, Weldment

1.0 INTRODUCTION

Metals are the most popular materials used in the construction and fabrication industries due to their physical, mechanical and chemical properties, which make them suitable for a wide range of engineering applications. In the course of equipment manufacturing and repairs, welding is one of the most important joining processes that are usually carried out. These are susceptible to corrosion in service as they are exposed to different environmental conditions. Corrosion of metals is recognized as a serious problem in most industries (Callister, 1997). Unprotected engineering structural materials, whether exposed to the atmosphere, or submerged in water, are susceptible to corrosion. The selection of metal for a particular technological process and application is dependent on the behavior under specific environment. The most commonly used material in manufacturing process favours carbon steel due to its wide availability, attractive cost and good properties of strength, ductility and weldability (Shrier, 1976; Bolton, 1994; Afolabi *et al.,* 2013; Gandy, 2007; and Nur and Shing, 2014).

Low carbon steel (LCS) is the most common form of steel as it provides material properties that are acceptable for many applications (Piccard, 1987). Shielded metal arc (SMA) welding is one of the world's popular welding processes practiced in the industry due to its simplicity (Kou, 2003). Many parameters affect the quality of welds and these varies for a range of welding processes and materials (Chang *et al*., 2004). Although, different grades and types of SMA electrodes are widely available in the market, they are made from different materials. Electrodes for LCS for instance are made by different manufacturers, and may have different formulation and properties. The choice of electrode for SMA depends on a numbers of factors including the weld material, welding position and the desired weld properties (Davis, 2006). Therefore, proper weld or filler

rod selection is important towards achieving a weld metal that will give a desired corrosion-resistance and strength characteristics.

According to Kou (2003), flux coated mild steel electrodes are the most common form of filler metal used in arc welding. The electrode wire rod is made of a material that is well-suited with the parent material being welded and is enclosed with a flux that shields the weld area from oxidation and pollution by giving out CO_2 gas during welding process. Meanwhile, it is well known that electrode formulation has influence on the mechanical properties of weldment It contributes to ascertain the usability of the electrode, the composition of the deposited weld metal, and the specification of the electrode (Hong *et al.*, 1996; Adetuji *et al.*, 2012; and Tewari *et al.*, 2010). Tewari *et al.* (2010) stated that the formulation of electrode core rod is very intricate. Although, it is not an accurate postulation, it is however, based on deep rooted metallurgy, chemistry, and physics blended with experience. Furthermore, alloying elements are added to the core rod basic elemental constituents, in order to enhance strength and provide specific weld metal deposit composition.

Nearly 90% of welding in the world is carried out by arc welding process, which generally involves melting and subsequent cooling (Tewari *et al.*, 2010). However, a flux-cored electrode acts as filler material, which makes the use of separate filler needless Therefore, SMA welding electrode constituent includes alloying metal, fluxes, deoxidizers and slag forming ingredients (Kou, 2003). For these reasons, this work relies upon the expertise of skilled welders to determine welding electrodes that would result in a good quality weld. Therefore, the focus of this work is to investigate the effect of shielded metal arc welding electrode on the mechanical properties of low carbon steel using SMA welding process. Additionally, the corrosion performance of the steel in 2.81 % NaCl solution using weight loss techniques, as well as the microstructural analysis of the studied electrodes is also investigated and evaluated.

2.0. MATERIALS AND METHOD

2.1 Materials and Preparation

Some of the materials used include welding electrodes (J-Wheel, China representing sample A; Oerlikon Nigeria, representing Sample B; J-Danish, India representing sample C) purchased from Samaru market, Zaria. Other materials used are Low carbon steel (5 mm thickness) purchased from Sabo market, Zaria, Nigeria.

Low carbon steel samples were cut manually using hack saw into various test samples of 7.5 x 5 cm^2, and 3 x 5 cm^2, giving double V-edge shape, and welded together with the different electrodes with AC SMA welding machine. Samples for impact test was given a notched of 0.3 mm depth at angle 45° to acts as stress concentration on the weldment.

Samples for weight loss corrosion were ground, polished using emery cloth of different grades (120 and 220) to obtain a mirror-like surface finish thereafter, cleaned with acetone. Furthermore, the specimens were dried in the air and weighed using digital electronic mass balance with ± 0.001g accuracy, immersed in 2.81 % NaCl solution for a total period of 504 hours with seven weight measurements taken at intervals of 72 hours and kept in fixed positions to prevent the effect of displacement as shown in **Figure 1**. Also, the rates of corrosion of the samples were evaluated in millimeter per year using the established relation by Callister (1997) as in Eq. (1).

$$Corrosion\ Rate\ (CR) = \frac{87.6 * W}{\rho * A * t}(mmpy) \quad (1)$$

where, W - weight loss in mg, ρ - metal density in gcm^{-3}, A - exposed area of the test specimen in cm^2, T - exposure period (hrs).

Figure 1: Corrosion Experimental Setup

Figure 2: Tensile Test Fractured Samples

2.2 Elemental and chemical Analysis

The as-received low carbon steel samples were subjected to spectrochemical analysis adopting the method of Fe-10-ASML in accordance with ASTM E415 standard using Optical Emission Spectroscopy (Model No: LMM05). The elemental analysis of the sourced electrodes was conducted in accordance with standard procedure using the mini pack-4 X-ray fluorescence (XRF) and Shimaxu Atomic Absorption spectrometry (AAS) respectively. The electrodes were dissolved in standard XRF solution before analyzing while AAS was used for determination of carbon contents only.

2.3 Tensile Test

Samples with dimension of 150 mm length and 50 mm breadth were extracted and subjected to tensile tests in accordance with the ASTM E8-04 standard using TUE-C-1000 Computerized Universal Testing Machine (Model 2009/654UA) at a loading rate of 1 $kNsec^{-1}$. The load versus extension graph was plotted and parameters such as the load and elongation at yield, yield stress, ultimate load and stress, percent reduction area and load before fractured were determined.

2.4 Hardness Test

The hardness values of the sourced low carbon steel (LCS) was obtained in accordance with the ASTM E18-07 standard using the Rockwell Identer Universal Hardness Testing machine, which had a digital display reading of scale F type (HRB Scale) with a diamond cone shape indenter, under minor and major loads (98.0665 N and 1838.7468 N) respectively.

2.5 Impact Testing

Impact tests of the sourced LCS were conducted according to ASTM A256; ISO 180 using the notched Izod impact tester of capacity 162.696 Nm.

2.6 Microstructural Analysis

The metallographic examinations of the LCS were done in accordance with ASTME 340 using the high resolution photographic visual metallurgical microscope with x100

magnification. The welded samples were carefully sectioned at different interface and polished with abrasive papers of successive finer grade (240, 320, 400, 600, and 800), and further swabbed in 2 % Nital solution.

3.0 RESULTS AND DISCUSSION

3.1 Elemental and Chemical Analysis

The elemental composition presented in **Table 1** indicated that iron constitutes highest concentration followed by manganese while carbon, chromium, copper and silicon, combined as inter-metallic compounds with iron in the alloy. Carbon plays a principal factor in weldabilty (Gandy, 2007; and Kou, 2003) and alloying of steel; therefore, ascertaining the chemical composition of the as-received samples for conformity to manufacturer's specification was important. The chemical and elemental compositions of the sourced electrodes and LCS used in this study are presented in **Tables 1 and 2**.

Electrode wire compositions are purposefully selected to match the metals being joined as the characteristics of the weld metal are primarily dependent on the alloy content of the filler rod and to a lesser extent on the degree to which the molten weld metal is protected from the environment (AISII, 2015). Manganese constitutes the highest amount of elemental composition in all the tested electrodes. Nickel and chromium were not present in sample C electrode. However, during the welding process, no difficulty was encounter in welding the LCS with the mild steel electrodes.

Table 1: Chemical Composition of As-received Low Carbon Steel

Element	Composition (%W)
C	0.137
Si	0.226
S	0.54
P	0.04
Mn	0.537
Cu	0.203
Sn	0.063
Cr	0.175
Sb	0.016
Fe	98.39
Others	<0.16

Table 2: Elemental Composition of Sourced Electrodes

Element	Composition (%W)		
	Sample A	Sample B	Sample C
C	0.07	0.07	0.06
Mn	1.28	1.31	1.19
S	0.002	0.018	0.011
P	0.003	0.02	0.017
Si	0.066	0.45	0.42
Cr	0.009	0.009	
Ni	0.03	0.008	

3.2 Tensile Strength

Figures 3 -.6 presented the graphs of load versus cross head travel (CHT) for each of the samples subjected to tensile tests. **Figure 3** (control specimen) revealed a directly

proportional trend of gradual increase in uni-axial load with a corresponding increase in extension. Thus, until the neck formed, the deformation was essentially uniform throughout the sample, but after necking all subsequent deformation took place at the neck region, which caused neck shrinkage and non-uniform geometry that altered the uniaxial stress state (Davis, 1998). The ultimate tensile stress (UTS) was 440.96 Nmm^{-2} with corresponding 46.52 % reduction in area and 60.80 % extension at fractured load point of 96.040 kN. Thus, visual observation showed an elastic-plastic transition with a typical cup and cone geometry fracture, which indicated that the sample was still ductile after the exposure (**Figure 3**).

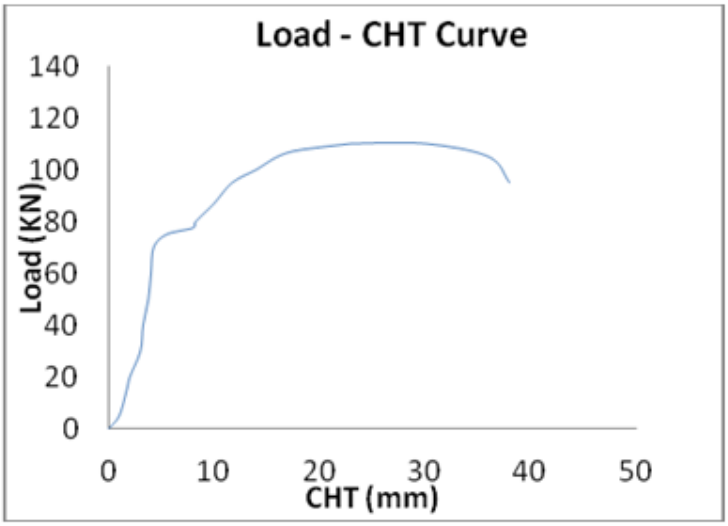

Figure 3: Load – CHT Curve Control Sample

Figures 4 - 6 presented the tensile evaluation of samples A and C. These show a decrease in ductility of the samples and an exemplarily trend of load versus CHT. Visual observation of the fractured surface showed a crystalline macrostructure. This indicated that the sample was brittle as failure occurred with lower plastic deformation as compared to the control (**Figure 3**). In comparison, samples A and C gave the lowest UTS (227.92 Nmm^{-2} and 231.88 Nmm^{-2}) with percent reduction areas of 6.94 and 8.00 %, at 41.70 and 41.53 kN fractured loads point. However, the small differences in their maximum and fractured loads could be ascribed to the low plastic deformation before fracture during their transition stage since iron oxides and pitting defects were found on the surface of the sample.

From the Load versus CHT curve in **Figure 5** (sample B), plastic deformation occurred before fracture of the sample. Visual observation of the fractured surfaces showed a fibrous macrostructure that completely fractured not only at the welded joint but also outside the welded zone. The weld gave the highest yield stress value of 352.96 Nmm^{-2} at UTS of 420.52 Nmm^{-2} and 18.1 % elongation among all samples extracted from the weldment.

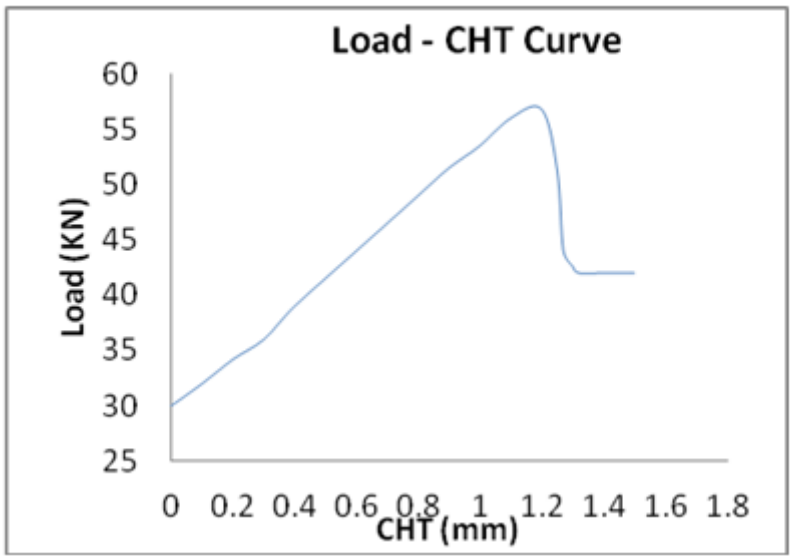

Figure 4: Load – CHT Curve Sample A

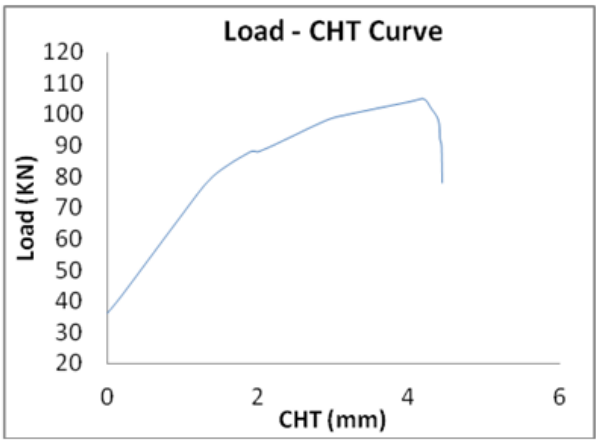

Figure 5: Load – CHT Curve Control Sample B

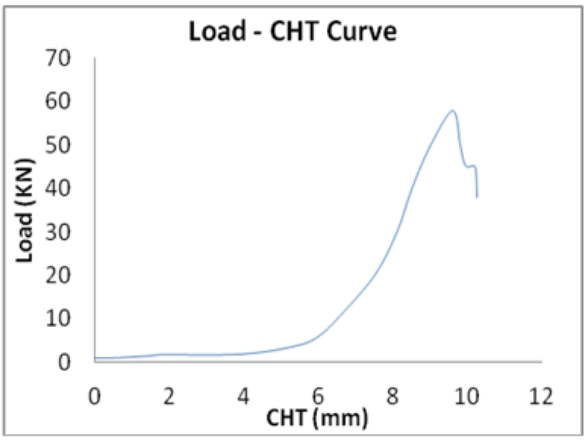

Figure 6: Load – CHT Curve Sample C

The investigation of the effects of the shielded metal arc welding electrodes on low carbon steel using the computerized universal tensile machine has been able to predict the behavior of the material under examination (**Figure 7**). Sample B weldment gave good properties and compared favourably with the unwelded (Cl: control) sample in all parameters evaluated (Tewari *et al.,* 2010). This would serve as a guide for skilled welders during filler rod selection of shielded metal arc welding electrode types in order to withstand failure under service conditions.

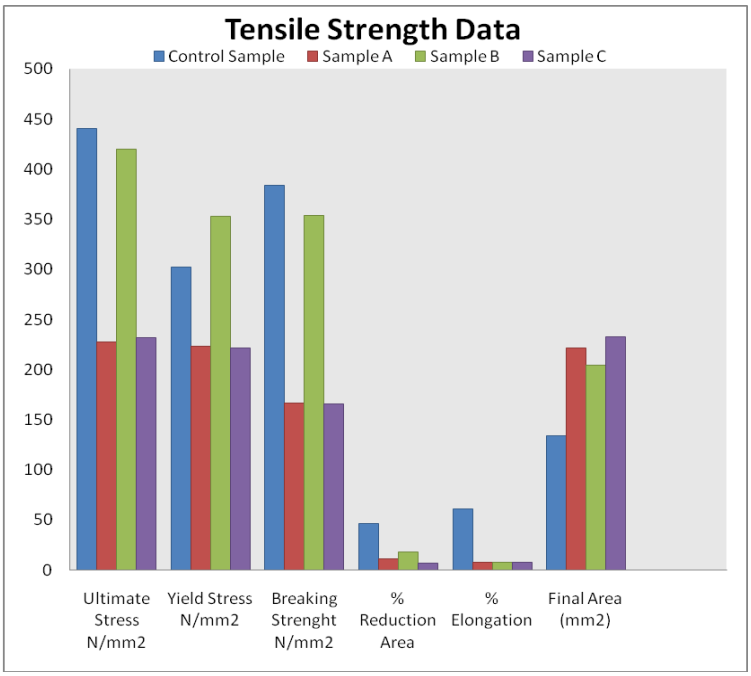

Figure 7: Tensile Parameters of the Samples

3.3 Hardness Value

Hardness values of welded and un-welded samples are presented in **Figure 8**. The trend showed that the average hardness values obtained at the weldment were relatively higher compared to the un-welded (control) samples and increases with exposure time in increasing order of Sample C > B > A. These variations could be credited to the small differences in formulations of the electrodes used (Higgins, 1993; Surian and Vedia, 1999). Sample C gave the highest average hardness value of 111.9 HRB at 504 hours immersion time in all test samples.

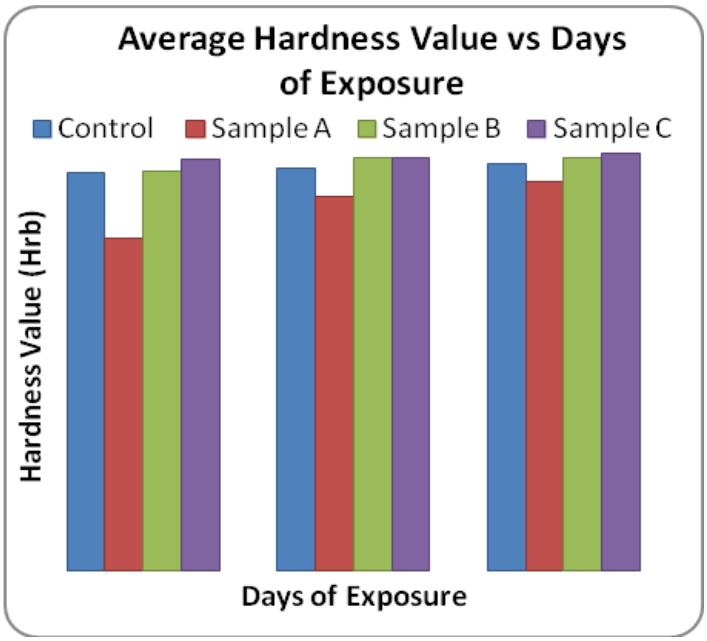

Figure 8: Hardness Value of the Samples

3.4 Impact Resistance

The impact resistance of welded and un-welded samples is presented in **Figure 9**. The impact resistance energy occurred in the following order C> A > B > Control (Cl: un-welded). This sequence is in accordance with that obtained from tensile tests.

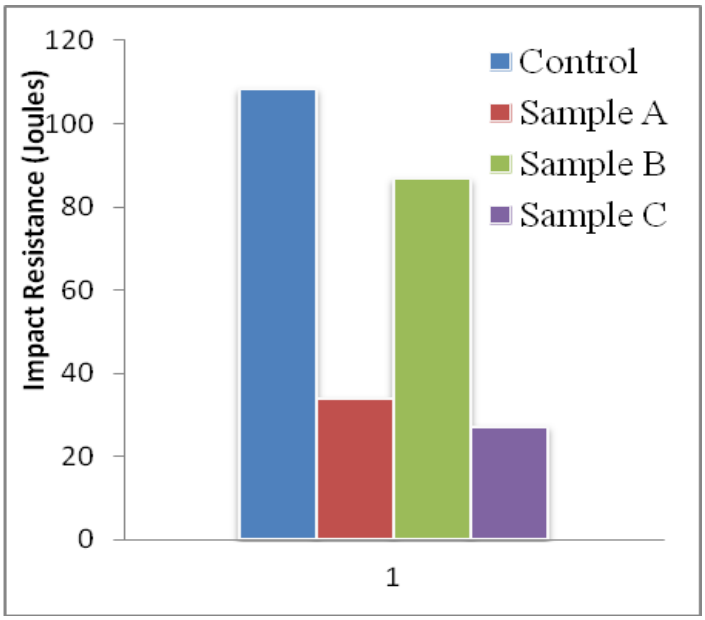

Figure 9: Impact Resistance of the Samples

3.5 Corrosion tests

Consistent corrosion was noticed in all the test coupons immersed in 2.81 % NaCl solution and the plots of the Weight Loss (WL) and Corrosion Rate (CR) as a function of exposure time are computed and presented in **Figures 10 and 11**. Weight loss and corrosion rates are in the following increasing order: Control < B < A < C. The high rate of corrosion obtained in sample C could be attributes to the absence of Cr and Ni in the composition of its electrode (**Table 2**).

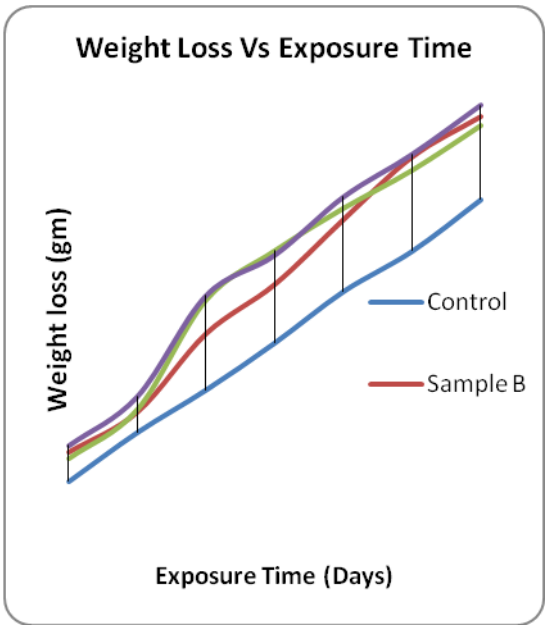

Figure 10: Variation of WL Vs ET

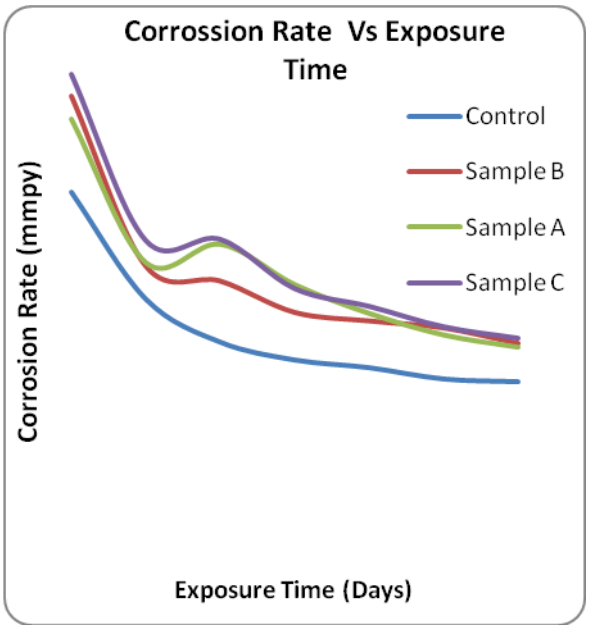

Figure 11: Variation of CR Vs ET

As observed from the trends in **Figure 11**, the corrosion rates decrease as the exposure times increased. These reductions could be attributed to formation of passive films on the samples surface at the onset of corrosion (Revie and Uhlig, 2008). The corrosion rates were, however, observed to fluctuate periodically. From the recorded corrosion rates, it is evident that the rate of corrosion for sample C in the environment increases with 0.00562 mmpy (0.09158 to 0.0972) and 0.0037 mmpy (0.09820 to 0.009857) on the 6^{th} and 9^{th} day of the exposure time respectively. This can be attributed to constant damage on the protective film formed in the chloride environment, which may be due to the formulation of electrode core rod (chromium and nickel) or increase in manganese composition in the weldment environment or the high concentration of manganese (Mn > 0.537) present in the parent metal (Glolam *et al.,* 2011; Hashimoto *et al.,* 2007).

3.6 Micro Analysis

Figures 12 – 14 shows the micrographs of samples A, B and C at different interface of sectioning.

Figures 12a, b and c show micrographs of sample A at different interfaces such as the base metal, weldment, and HAZ respectively. The microscopic studies revealed that the HAZ contains coarse grains of heterogeneous and unevenly ferrite phase that grows along a certain preferred crystallographic direction adjacent to the weld fusion zone, to produce grains larger than those in the base metal. Several studies (Shing, 2014; Adetunji *et al*., 2012; Tewari, *et al.,* 2010; Hashimoto, *et al.,* 2007) have shown that welded structures have heterogeneity in the heat affected zone (HAZ) induced by the welding process (Davis, 1998). Microstructural changes across sectioning of the welds depend largely on the filler material used (Charde, 2012).

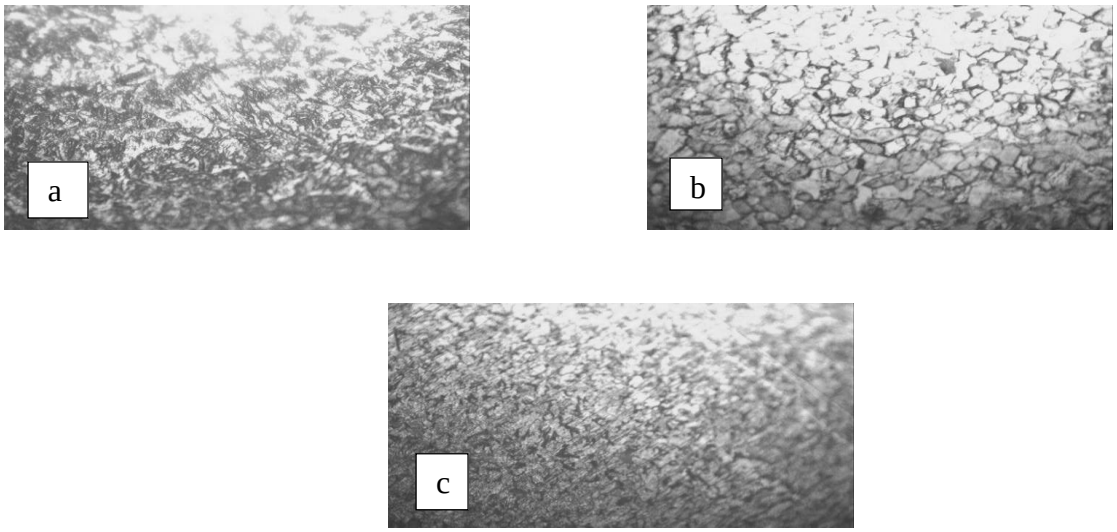

Figures 12: Micrographs of sample A at HAZ (a), Parent metal (b), weldment (c).

The micrographs of the welded samples B and C are presented in **Figures 13a - c and 14a – c**. They revealed the presence of homogeneous microstructure in the HAZ and weld area which has a greater significance on the mechanical properties of welded structures.

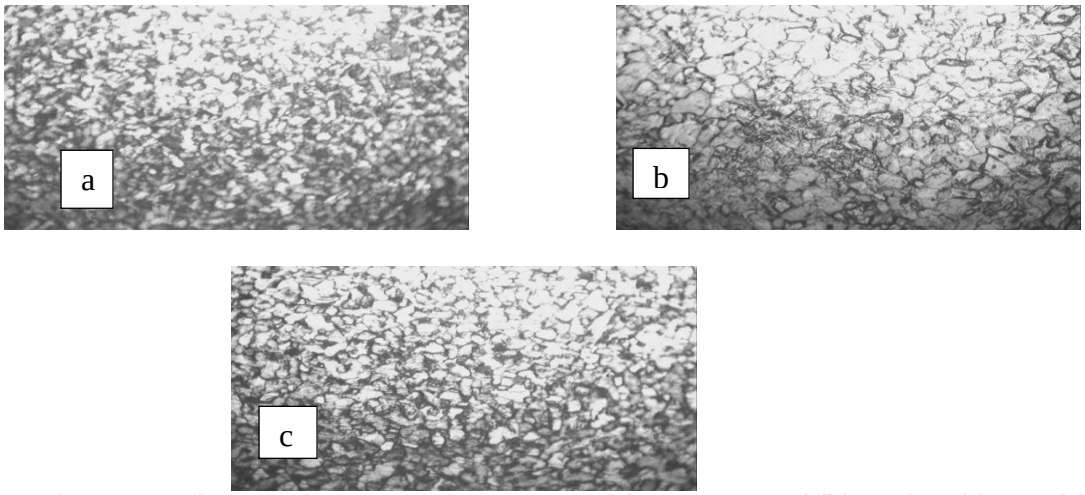

Figure 13: Micrographs of Samples B at HAZ(a), Parent Metal (b), and Weldment (c).

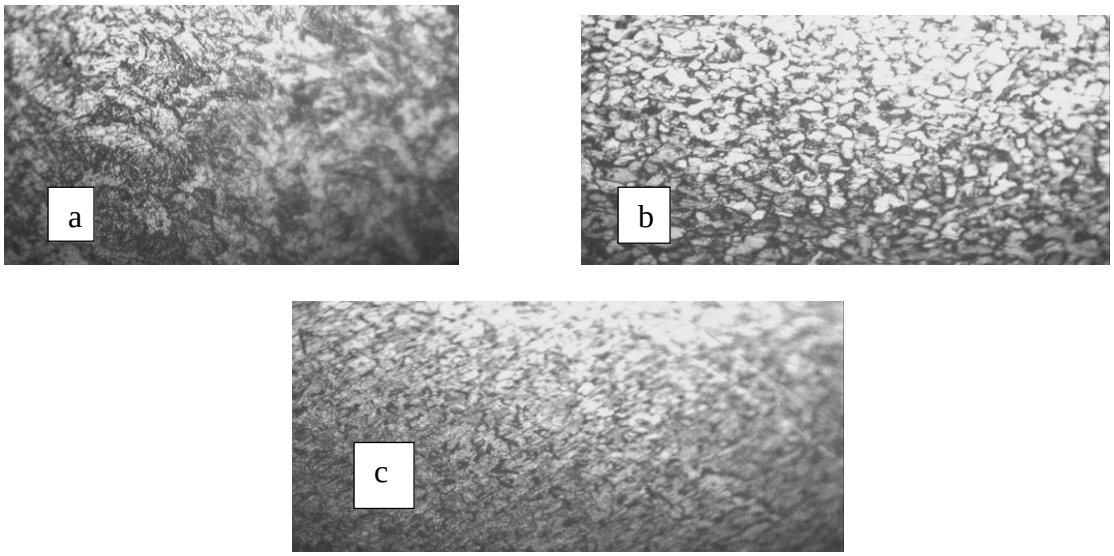

Figure 14: Micrographs of Samples C at HAZ(a), Parent Metal (b), and Weldment (c).

4.0 CONCLUSION

The conclusions drawn from this research work are as follows:

1) Uniform corrosion was observed for LCS, however, there was an increase in metal loss and decrease in the corrosion rate as the exposure time increased.
2) The type of electrode used in SMA welding process affects the quality of weld and corrosion resistance at the weld joint.
3) Weldment where sample B (Oerlikon electrode produced in Nigeria) showed the best chemical and mechanical properties amongst the three electrodes. This is in agreement with theoretical expectation based on its composition.

ACKNOWLEDGEMENT

We would like to acknowledge the Head of the Quality Control (QC) Department of Abuja Steel Mills for provision of Computerized Universal Testing machine and Mr. Ezekiel of the Department of Pharmaceutical Microbiology, Ahmadu Bello University, Zaria, Nigeria for their assistance.

CONFLICT OF INTEREST

All the parties involved in this research work declared there is no conflict of interest.

REFERENCES

Adetunji, K. O, Adekunle, T. O., Olasupo, O, and Bankole, A., (2012). ComparativeEvaluation of Flux Coated Mild Steel Electrodes in Nigeria. AU *Journal of Technology*, Thailand, 201 – 204.

Afolabi, A. S., Ngwenya, T. G., Sanusi, O. K. and Abdulkareem, A. S., (2013). Stress Corrosion Cracking of a Mild Steel in Orange Juice. Proceeding of the World Congress on Engineering, Vol. 1: 13 – 20 London, UK, July 3- 5, 2013.

American Iron and Steel Institute (1988). AISII Designers Handbook Series - Welding of Stainless Steels and Others Joining Methods, Nickel Development Institute, August 1988, www.nidi.org. Accessed on September 9, 2015

Bolton, W., (1994). Engineering Materials Technology, 2nd Edition, B. H. Newness Ltd, Oxford, London.

Callister, W. D., (1997). Materials Science and Engineering: An Introduction, 7th Edition, John Wiley and Sons Inc., New York, USA

Chang, P. Y., Heung, W. Yun, M. and Green, P. G., (2004). Report on Improving Welding Toxic Metal Emission Estimates in California, University of California, Davis, 14th July 2004.

Charde, N., (2008). Effects of Electrode Deformation of Resistance Spot Welding on 3014 Austenitic Stainless Steel Weld Geometry. *Journal of Mechanical Engineering and Sciences*, 3, 261 – 270.

Davis, J. R., (1998). Metal Handbook, 2nd Edition, Taylor and Francis, CRC Press, United Kingdom.

Davis, J.R., (2006). Basic Understanding of Weld Corrosion, Corrosion of Weldments, ASM International, New York, USA.

Gandy, D., (2007). Carbon Steel Handbook. Electric Power Research Institute (EPRI), Palo Alto

Glolam, R. R., Hamed, G., Gholam, R. Z., Davood, Z., Mohsen, S. and Hossein, M., (2011). Study of Corrosion of High-Mn Steels with Mo in 3.5 % NaCl Solution. *Journal of International Conference on Advance Materials Engineering*, 15, 36-39.

Hashimoto, K., Asami, K., Kawashima, A., Habazaki, H and Akiyama, E., (2007). The Role of Corrosion-resistant Alloying Elements in Passivity, *Corrosion Science*, 49, 42 – 52.

Higgins, R. A. (1993). Engineering Metallurgy: Part 1, Applied Physical Metallurgy, Edward Arnold, London

Hong K., Weckman, D. C., and Strong, A. B., (1996). “Trends in Welding Research”, ASM International, Materials Park, USA, pp. 399-404.

Kou, S., (2003). Welding Metallurgy, 2nd Edition, John Wiley and Sons, Inc., New York, USA.

Nur, A. A. and Shing, S. N., (2014). Investigation of Effects of MIG Welding on Corrosion Behaviour of AISI 1010 Carbon Steel. *Journal of Mechanical Engineering and Sciences* 7, 1168-1178.

Piccard, G.S., Lefebure, M. H., and Tremillion, C., (1987). Proceeding of Joint Symposium on Molten Materials Salt, Vol. 81, pp.10 - 28. Japan, 19 87.

Revie, R. W., and Uhlig, H., (2008). Corrosion and Corrosion Control, 4th Edition, Wiley, New York, 200

Shrier, L. L., (1976). Corrosion, 2nd Edition, Newnes-Butterworth, London, United Kingdom

Surian, E. S., and Vedia, L. A., (1999). All-Weld-Metal Design for AWS E10018M, E11018M and E12018M Type Electrodes, Welding Research Supplement, June 1999, pp 218s- 228s

Tewari, S. P., Gupta, A., and Prakash, J., (2010). Effect of Welding Parameters on the Weldability of Material. *International Journal of Engineering Science and Technology*, 2 (**4**): 512-551